UCLA
UCLA Electronic Theses and Dissertations

Title

Exploring the Cytotoxic Efficacy of Supercharged NK Cells in Uterine Cancer Models

Permalink

https://escholarship.org/uc/item/9n11p4w9

Author

Sher, Edward

Publication Date

2024

Peer reviewed|Thesis/dissertation

eScholarship.org Powered by the California Digital Library
University of California

UNIVERSITY OF CALIFORNIA

Los Angeles

Exploring the Cytotoxic Efficacy of Supercharged NK Cells in Uterine Cancer Models

A thesis submitted in partial satisfaction of the requirements for the degree

Master of Science in Oral Biology

by

Edward Sher

2024

© Copyright by

Edward Sher

2024

ABSTRACT OF THE THESIS

Exploring the Cytotoxic Efficacy of Supercharged NK Cells in Uterine Cancer Models

by

Edward Sher

Master of Science in Oral Biology

University of California, Los Angeles, 2024

Professor Anahid Jewett, Chair

Natural Killer (NK) cells are essential components of the immune system, responsible for combating tumors and virulent pathogens. This thesis explores the effects of supercharged NK (sNK) cells, expanded through osteoclast co-culture, on uterine cancer cell lines and in vivo tumor models. The study focuses on comparing the cytotoxicity and functionality of sNK cells expanded using live and sonicated osteoclasts, investigating their effectiveness against poorly differentiated uterine cancer cell lines, and assessing their impact on tumor progression in humanized BLT (huBLT) mouse models.

In Chapter 1, we establish the functional differences between sNK cells expanded through live and sonicated osteoclasts. Our results show that live osteoclast-expanded sNK cells

exhibit superior cytotoxicity and higher IFN-γ secretion, indicating a more potent immune response.

Chapter 2 investigates the cytotoxicity of sNK cells against the poorly differentiated AN3CA and well-differentiated HEC-1B uterine cancer cell lines. Our findings reveal that sNK cells exhibit higher cytotoxicity against AN3CA cells, comparable to their effect on stem-like cancer cells (OSCSC), while showing lower cytotoxicity against HEC-1B cells. Real-time cytotoxicity monitoring further supports these results, highlighting the dynamic and enhanced killing capability of sNK cells. Additionally, sNK cells demonstrate superior performance compared to primary NK (pNK) cells treated with IL-2 or IL-2+sAJ4, underscoring the enhanced efficacy of osteoclast-expanded sNK cells.

In Chapter 3, we assess the in vivo efficacy of sNK cells in targeting AN3CA tumor progression in huBLT mice. The results indicate a significant reduction in tumor burden in sNK-treated mice, with decreased tumor weight and volume compared to controls. Furthermore, increased IFN-γ secretion levels in sNK-treated mice suggest a reinvigoration of the immune system's capacity to combat cancer, potentially reversing tumor-induced immunosuppression.

Overall, this thesis demonstrates the enhanced cytotoxic capabilities and therapeutic potential of sNK cells in targeting poorly differentiated and aggressive cancer cells. The findings support the development of sNK cell-based immunotherapies as a promising approach for treating aggressive cancers and improving patient outcomes.

The thesis of Edward Sher is approved.

Ichiro Nishimura

Nicholas A. Cacalano

Anahid Jewett, Committee Chair

University of California, Los Angeles

2024

DEDICATION

I dedicate this thesis primarily to my parents,

Anthony

and

Fiona

who have given me limitless educational opportunities, and to my friends and family who have supported me throughout this time, in the faith that this research may, in some way, contribute to the advancement of cancer immunotherapy.

Table of Contents

Acknowledgment

I would like to extend my deepest gratitude to all those who have supported and guided me throughout my thesis journey. First and foremost, I would like to thank my mentor, Dr. Anahid Jewett, for her support, insightful guidance, and constant encouragement. Her expertise and dedication have been instrumental in the completion of this work. I am also grateful to my committee members, Dr. Ichiro Nishimura and Dr. Nicholas Cacalano, for their valuable feedback, constructive criticism, and the time they have invested in my research. Their guidance has significantly enhanced the quality of my work.

To my lab members, Po-Chun Chen, Sara Huerta, Janet Pham, Tiran Sargsyan, Sonia Virk, Jillian Poulsen, and Derrick Mardirosian, I extend my heartfelt thanks. Your assistance, collaboration, and friendship have been vital to my progress. Thank you for being there during challenging times, for offering your expertise, and for contributing to a supportive and stimulating research environment.

Each one of you has played a crucial role in my academic journey, and I am sincerely appreciative of your support and dedication. Thank you all for your invaluable contributions.

Introduction

Natural Killer Cell

Natural Killer (NK) cells, essential constituents of the immune system, are lymphocytes originating from the bone marrow, embodying characteristics that allow them to act as the body's frontline defense against tumors and virulent pathogens. These cells, notable for their large granules filled with potent cytotoxic molecules, represent approximately 5 to 15% of the lymphocytes in human blood [1]. Their identification is facilitated by distinct surface markers, notably CD16 and CD56, with the absence of CD3 that sets them apart from T cells [2]. NK cells thrive within peripheral blood mononuclear cells (PBMCs), playing a crucial role in the innate immune system, where they directly engage and neutralize threats and shape the adaptive immune response through their production of cytokines [3].

NK cell-mediated cytotoxicity is largely dependent on the action of perforin, which is a protein known to pierce through cell membranes, and granzyme B, an enzyme that acts as a serine protease [4]. The functionality of NK cells is delineated into two main subsets, characterized by their surface marker expression and inherent roles. The CD16+ CD56dim subset, constituting the majority of NK cells in circulation, is primarily associated with direct cytotoxic activities against compromised cells [5]. Conversely, the CD56bright subset, though less prevalent, is essential for cytokine secretion, influencing both innate and adaptive immune mechanisms [6]. The balance between activating and inhibitory signals received through receptors such as NKG2D, NKp44, and KIR2 dictates the cytotoxic response of NK cells, ensuring targeted action against malignancies while sparing healthy tissues [7]. Beyond their innate cytolytic functions, NK cells possess the ability to induce differentiation in cancer stem cells, particularly those within poorly differentiated tumors, through the secretion of cytokines like IFN-γ and TNF-α [8]. This capacity highlights the

versatility of NK cells in tumor surveillance and underscores their potential in advancing cancer immunotherapy strategies.

Endometrial Cancer

Endometrial cancer (EC), the most common form of uterine cancer, originates from the endometrium, the lining of the uterus. Globally, EC ranks as the fourth most common cancer among women, with its incidence rising by approximately 20%, affecting about 1 in 37 women in their lifetime [9]. Traditionally seen in postmenopausal women, there's a noticeable increase in younger women, attributed to early-onset obesity and hyperinsulinemia [10].

Despite being often detected at an early stage due to symptoms like irregular vaginal bleeding, EC remains a significant health burden for several reasons. Firstly, the incidence and mortality rates of this cancer are on the rise. Type II endometrial cancer, which is high-grade and often detected at an advanced stage, accounts for a substantial proportion of all deaths from endometrial cancer [11]. This type's aggressive nature and late detection contribute significantly to the overall health burden of the disease, with an estimated 13,030 deaths anticipated in 2023 out of 66,200 new cases [12]. This places a spotlight on the necessity for effective diagnostic and therapeutic strategies. Among the established cell lines AN3CA, ECC-1, HEC1A, HEC1B, and Ishikawa, we specifically chose AN3CA and HEC-1B to examine their interactions with NK cells.

Differentiation of Tumors

Stem-like/poorly differentiated and well-differentiated tumors represent contrasting states

of cancer cell maturity, with significant implications for treatment and prognosis. Stem-like/poorly differentiated tumors are characterized by a lack of mature cellular features and often exhibit aggressive growth patterns, making them less responsive to conventional chemotherapies. These tumors tend to grow rapidly, forming large masses, and show lower expression of differentiation markers like MHC-class I, CD54, and PD-L1 [13]. In contrast, well-differentiated tumors resemble their tissue of origin more closely, displaying higher expression of differentiation antigens and are generally more susceptible to chemotherapeutic agents.

Research has shown that the differentiation stage of cancer cells influences their interaction with the immune system, particularly Natural Killer (NK) cells [13]. Poorly differentiated tumors are preferentially targeted by NK cells, which can also induce differentiation in these tumors, thereby increasing their susceptibility to drug-mediated cell death. This highlights the potential of NK cell-based therapies to not only directly lyse cancer cells but also to enhance the effectiveness of conventional treatments by promoting tumor differentiation. For instance, supercharged NK cells, when used in combination with chemotherapy or immunotherapy, have shown promise in reducing tumor size and enhancing NK cell function in experimental models, underscoring the importance of considering tumor differentiation in designing treatment strategies.

AN3CA

The AN3CA cell line, utilized in EC research, is classified as poorly differentiated [14]. Poor differentiation indicates that the cells exhibit low similarity to normal endometrial cells, reflecting a high grade of malignancy and aggressive tumor behavior [15]. AN3CA exhibits migratory properties and is tumorigenic in nude mice [16]. Such characteristics make AN3CA a valuable model for studying advanced disease stages and testing therapeutic strategies targeting

aggressive cancer forms. While NK cells have been extensively studied for their cytotoxic capabilities against various cancers, specific research on NK cells' effectiveness against the AN3CA EC cell line is not directly highlighted in the available literature.

HEC-1B

The HEC-1B cell line is a specific substrain of HEC-1-A, isolated for its distinct characteristics including a stationary growth phase observed between the 135th and 190th days in culture [17]. This substrain exhibits morphological changes upon recovery, appearing flatter and adopting a more pavement-like pattern compared to the parent line. HEC-1B forms moderately well-differentiated adenocarcinomas in nude mice and steroid-treated hamsters, consistent with grade II endometrial carcinoma [15]. Distinct from AN3CA, known for its aggressive and poorly differentiated characteristics, HEC-1B is often utilized in studying hormone responses and gene expression.

Osteoclasts

Osteoclasts are derived from hematopoietic stem cells and they play a crucial role in bone tissue maintenance, repair, and remodeling by resorbing bone tissue. This process, along with osteoblast bone formation, is essential for bone homeostasis [18, 19, 20]. Osteoclast maturation is stimulated by osteoblasts expressing RANKL, with their interaction facilitated by firm adhesion through ICAM-1 [19]. Previous studies demonstrated that osteoclasts express ligands for receptors present on activated NK cells, such as ULBP-1, ULBP-2/5/6, and ULBP-3, while lacking expression of MIC-A, MIC-B, or MHC class I-like ligands for NKG2D [21].

Previous research has highlighted osteoclasts as significant activators of NK cell expansion and function compared to dendritic cells and monocytes [22]. Osteoclasts secrete IL-12, IL-15, IFN-γ, and IL-18, known to activate NK cells, and express important NK-activating ligands [23].

Super-Charged NK Cells (Osteoclast-expanded NK Cells)

Super-charged NK cells (sNK) are NK cells that have undergone an expansion process facilitated by osteoclasts, significantly enhancing their functional capabilities [24]. This expansion leads to a marked increase in their proliferation rate, cytotoxicity against cancer cells, and an increase in the secretion of IFN-γ, a critical cytokine in immune response modulation [25]. Unlike primary NK cells (pNK) from PBMCs, sNK cells maintain their enhanced functions even when targeting challenging targets like oral squamous carcinoma stem-like cells (OSCSCs) or poorly differentiated tumors [26]. sNK cells exhibit a higher expression of activating receptors such as NKG2D, NKp44, NKp46, and granzyme B, which contribute to their increased cytotoxicity and enhanced IFN-γ secretion [24]. Compared to primary NK (pNK) cells, sNK cells are more polyfunctional, showcasing superior multi-faceted immune responses. This makes sNK cells a promising field for research and application in cancer immunotherapy, offering a potential for more effective targeting of cancer cells.

OSCSC (Oral Squamous Carcinoma Stem Cells)

Oral Squamous Carcinoma Stem Cells (OSCSCs) are a specialized subset of cells found within oral squamous cell carcinomas, known for their lower differentiation and higher susceptibility to NK cell-mediated cytotoxicity. Unlike differentiated carcinoma cells, OSCSC exhibits slight B7H1 and EGF-R expression and none of MHC-Class II or CD90 [27]. Yet, OSCSC

expresses high levels of CD133, CD44, EpCAM, CD26, and CD338, making them prone to NK cell cytotoxicity and able to stimulate IFN-γ secretion.

Humanized Mouse Model

The Humanized Mouse Model, utilized to study Cancer Stem Cells (CSCs) and their ability to initiate human tumors, exhibits varied NK cell impairment across strains like nude, NOD-scid, and NSG [28]. Questions persist about immune subsets' roles in cancer control, motivating the use of humanized mice with restored immune systems for better assessment [29].

Efforts to develop mice with fully reconstituted human immune systems are ongoing, primarily using NSG or NRG strains due to their severe immunodeficiency [30, 31]. Various methods exist for humanizing mice, such as injecting them with human PBMCs or isolating CD34+ progenitor cells for transplantation into NSG mice [28, 32].

Among these methods, the BLT humanized mouse model (hu-BLT) is the most notable [33]. It involves surgically implanting human fetal liver and thymus tissue under the renal capsule of NSG mice, followed by CD34+ cell injection [28, 33]. This model allows for human T cell development in the presence of a human thymus, resulting in functional CD4+ and CD8+ T cells with human MHC restriction [34, 35]. BLT mice also exhibit mucosal immunity and robust human leukocyte reconstitution, making them a promising tool for studying human immunity and cancer [36].

Thesis Outline

Specific Aim 1: Evaluating the Expansion and Cytotoxicity of sNK Cells: A Comparative Analysis of Live and Sonicated Osteoclast-Derived Effects

- Sub-aim 1: Quantitative Comparison of sNK Cell Cytotoxicity through Chromium Release Assay
- Sub-aim 2: Comparison of sNK Cell Activity through Real-Time Cytotoxicity Monitoring
- Sub-aim 3: Comparative Analysis of IFN-γ Expression of sNK

Specific Aim 2: To investigate and compare the lysing capacity of supercharged NK (sNK) cells and primary NK cells against Uterine Cancer Stem-like and Differentiated Cell Lines AN3CA and HEC-1B

- Sub-aim 1: Compare the cytotoxicity of sNK cells against AN3CA and HEC-1B cell lines
- Sub-aim 2: Compare the cytotoxicity of sNK cells with treated pNK cells
- Sub-aim 3: Real-time monitoring of NK cell-mediated cytotoxicity

Specific Aim 3: In Vivo Efficacy of sNK Cells in Targeting AN3CA Tumor Progression in huBLT mice Models

- Sub-aim 1: In vivo efficacy of sNK cells in targeting AN3CA tumor progression
- Sub-aim 2: Analyze the immune response in sNK-treated huBLT mice

Materials and Methods

Cell lines, reagents, and antibodies

Human immune cells were cultured in RPMI 1640, supplemented with 10% fetal bovine serum (FBS) (Gemini Bio-Products, CA). Oral Squamous Cancer Stem Cells (OSCSCs) were isolated from oral cancer patient tongue tumors at UCLA School of Medicine and cultured in RPMI 1640 supplemented 10% Fetal Bovine Serum (FBS) (Gemini Bio-Products, CA), 1.4% antibiotic antimycotic, 1% sodium pyruvate, 1.4% non-essential amino acids, 1% L-glutamine, 0.2% gentamicin (Gemini Bio-Products, CA, USA), and 0.15% sodium bicarbonate (Fisher Scientific, PA, USA). Endometrial cancer cell lines AN3CA and HEC-1B were purchased (ATCC, Manassas, VA) and cultured in EMEM medium with 10% FBS and 1% penicillin and streptomycin (Gemini Bio-Products, CA, USA). Osteoclasts were cultured with Alpha-MEM medium (Life Technologies, CA) supplemented with 10% FBS (Gemini Bio-Products, CA). Recombinant IL-2 was obtained from NIH-BRB. Antibodies used for flow cytometry– isotype control, CD45 (human), CD3, CD4, CD16, CD56, CD8, CD14, and CD19 – were purchased from Biolegend (San Diego, CA). Human NK purification kits were obtained from Stem Cell Technologies (Vancouver, BC, Canada).

Purification of NK Cells from Human Peripheral Blood

Written informed consents approved by UCLA Institutional Review Board (IRB) were obtained from healthy blood donors and all the procedures were approved by the UCLA-IRB. The Ficoll-Hypaque technique was used to fractionate the red blood cells and the white cloudy layer, also known as the buffy coat. The buffy coat contains Peripheral Blood Mononuclear Cells (PBMC), which were harvested, washed, and re-suspended in RPMI 1640 (Invitrogen by Life

Technologies, CA) supplemented with 10% FBS. NK cells were negatively selected and isolated from PBLs using the EasySep® Human NK cell enrichment kit purchased from Stem Cell Technologies (Vancouver, BC, Canada). The isolated NK cells were stained with anti-CD45, anti-CD16, anti-CD56, and anti-CD3 antibodies to ensure at least 90% cell purity through flow cytometry analysis. Purified NK cells were cultured in RPMI Medium 1640 supplemented with 10% FBS (Gemini Bio-Products, CA), 1% antibiotic antimycotic, 1% sodium pyruvate, and 1% MEM non-essential amino acids (Invitrogen, Life Technologies, CA).

Generation of Osteoclasts from Human Peripheral Blood

Written informed consents, approved by UCLA Institutional Review Board (IRB) were obtained from healthy blood donors, and all procedures were approved by the UCLA-IRB. After 1-2 hours of incubation of PBMC in culture dishes, the adherent subpopulation of PBMCs was detached from the tissue culture plates. Monocytes were purified using the EasySep® Human monocyte cell enrichment kit obtained from Stem Cell Technologies (Vancouver, BC, Canada). Based on flow cytometric analysis of CD14 the antibody-stained, enriched monocyte cells, the monocyte population was found to have at least 95% purity. Monocytes were cultured using alpha-MEM medium containing M-CSF (25 ng/mL) and RANKL (25 ng/mL) for 21 days, and the medium was refreshed every 3 days.

Sonication

Osteoclasts and probiotics were sonicated to disrupt cellular membranes and release the cell contents, effectively inducing cell death. A homogeneous population of sonicated osteoclasts and probiotics were thus obtained.

Live osteoclasts were counted and suspended in alpha-MEM medium supplemented with 10% fetal bovine serum (FBS) (Gemini Bio-Products), reaching a final concentration of 10^6 cells/ml. After every five pulses, a sample was taken and examined under a microscope until at least 80% of the cell wall was dissolved. The sample was then sonicated for 20 seconds while kept on ice, followed by a 30-second incubation on ice. This sonication process was repeated 15 times to ensure complete sonication.

AJ4 is a combination of 7 different strains of gram-positive probiotic bacteria (*Streptococcus thermophiles, Bifidobacterium longum, Bifidobacterium breve, Bifidobacterium infantis, Lactobacillus acidophilus, Lactobacillus plantarum, Lactobacillus casei, and Lactobacillus bulgaricus*), elected for their superior ability to activate NK cells. AJ2 was weighed and resuspended in RPMI Medium 1640 containing 10% FBS at a concentration of 10mg per 1 mL. The bacteria was thoroughly vortexed, then sonicated on ice for 15 seconds, at 6 to 8 amplitude. Sonicated samples were then incubated for 30 seconds on ice. After every five pulses, a sample was taken to observe under the microscope until at least 80 percent of cell walls were lysed. It was determined that approximately 20 rounds of sonication/incubation on ice, were conducted to achieve complete sonication. Finally, the sonicated samples (sAJ2, osteoclasts) were aliquoted and stored in a -80 ºC freezer.

Surface staining and Flow cytometry analysis

Staining was performed by staining the cells with antibodies as described previously. Briefly, all samples (4×10^4) were stained with 100µL of 1% BSA-PBS (Gemini Bio-Products, CA) and pre-determined optimal concentration of desired fluorochrome (PE, FITC or PEcy5)

conjugated antibodies. The samples were then incubated at 4°C for 30 min. The sample was washed and resuspended with 1% BSA-PBS. For the cell death assay, 3 x 10^4 cells in 100 µl of cold 1% BSA-PBS were stained with 8 mg/ml propidium iodide and reconstituted to a final volume of 200 µl with BSA-PBS. Attune NxT flow cytometer (Thermo Fisher Scientific, Waltham, MA) and FlowJo v10.4 (BD, Oregon, USA) were used for data analysis.

Expansion of NK Cells

human NK cells were purified and activated using rhIL-2 (1000 U/ml) and anti-CD16 monoclonal antibody (3 ug/ml) for 18-20 hours. Subsequently, the activated NK cells were co-cultured with osteoclasts and sAJ2 in a specific ratio of 2:1:4 (NK cells:osteoclasts:sAJ2). The culture medium was replenished with rhIL-2 every three days to maintain optimal conditions.

^{51}Chromium Release Cytotoxicity Assay

Chromium-51 (^{51}Cr) was obtained from Perkin Elmer (Santa Clara, California) for use in the standard ^{51}Cr release cytotoxicity assay. ^{51}Cr release cytotoxicity assay was employed to assess the cytotoxic function of NK cells in the experimental cultures. The assay was performed by incubating effector cells (1x10^5 NK cells/well) and ^{51}Cr–labeled target cells (5x10^5 OSCSC/HEC-1B/AN3CA) for four hours at four (5:1; 2.5:1; 1.25:1; 0.625:1) to six serial dilutions (5:1; 2.5:1; 1.25:1; 0.625:1; 0.3125:1; 0.15625:1). Following incubation, target cells were washed twice to remove excess unbound 51Cr. 51Cr-labeled target cells were aliquoted into the 96-well round bottom microwell plates containing effector cells at a concentration of 1x10^4 cells/well at a top effector: target (E:T) ratio of 5:1. After a 4-hour incubation period, the supernatant of each sample was harvested and the released radioactivity was measured using a gamma counter. The total

release (containing ^{51}Cr-labeled target cells) and spontaneous release (supernatants of target cells alone) values were recorded to calculate the percentage of specific cytotoxicity. The percentage-specific cytotoxicity was calculated using the following formula:

$$\%\ Cytotoxicity\ = \frac{Experimental\ cpm - Spontaneous\ cpm}{Total\ cpm - Spontaneous\ cpm}$$

Lytic unit (LU) $30/10^6$ is calculated by using the inverse of the number of effector cells needed to lyse 30% of tumor target cells × 100.

Enzyme-Linked Immunosorbent Assays (ELISAs)

Human ELISA kit for IFN-γ was purchased from Biolegend (San Diego, CA) to measure the IFN-γ levels in cell culture. The assay was conducted as described in the manufacturer's protocol. Briefly, 96-well EIA/RIA plates were coated with diluted capture antibody corresponding to target cytokine and incubated overnight at 4°C. After 16-18 hours of incubation, the plates were washed 3 times with wash buffer (0.05% Tween in 1xPBS) and blocked with assay diluent (1%BSA in 1xPBS). The plates were incubated for 1 hour at room temperature, on a plate shaker at 200rpm; plates were washed 3 times following incubation. Then, 100uL of standards and samples collected from each culture were added to the wells and incubated for 2 hours at room temperature, on the plate shaker at 200rpm. After incubation, plates were washed 4 times, loaded with detection antibody, and incubated for 1 hour at room temperature, on the plate shaker at 200rpm. After 1 hour of incubation, the plates were washed 3 times; wells were loaded with Avidin-HRP solution and incubated for 30 minutes at room temperature, on the plate shaker at 200rpm. After washing the plates 5 times with wash buffer; 100uL of TMB substrate solution was added to the wells and plates were incubated in the dark until they developed a desired blue color (or up to 30 minutes). Then, 50uL of stop solution ($2NH_2SO_4$) was added per well to stop the

reaction. Finally, plates were read in a microplate reader, at 450nm to obtain absorbance values (Biolegend, ELISA manual).

Analysis of human AN3CA cell growth in humanized mice

Animal research was performed under the written approval of the UCLA Animal Research Committee (ARC) in accordance to all federal, state, and local guidelines. Humanized-BLT (hu-BLT; human bone marrow/liver/thymus) mice were prepared and maintained in the animal facilities at UCLA under protocols approved by the UCLA as previously described [37, 38].

In vivo growth of human endometrial carcinoma stem cells (AN3CA) was determined by orthotopic cell implantation of tumor cells into hu-BLT mice. To establish orthotopic tumors, mice were first anesthetized using an isoflurane setup, and AN3CA were then transferred by direct injection of $1x10^6$ cells mixed with 10 µL HC Matrigel (Corning, NY,USA) directly into the uterus. Immediately before tumor cell injection, 5.0-mg/kg carprofen was injected subcutaneously, and this injection was repeated every 24 hours for 48 hours.

Following injection of tumor cells, all mice were continuously monitored for disease progression every other day. Mice were observed for overall signs of morbidity, such as loss of weight, ruffled fur, hunched posture, and immobility. Seven days after tumor implantation selected hu-BLT mice received $1.5x10^6$ human expanded NK cells via tail vein (IV) injection. Mice were euthanized in 6 weeks when signs of morbidity were evident. Tumor volumes were determined using the formula:

$$volume = \frac{Length \times Width^2}{2} \times \frac{3\pi}{4}$$

Cell dissociation and cell culture from tissues of tumor bearing hu-BLT mice

At the end of the experiment, mice were euthanized and the tumor, liver, bone marrow, spleen and blood were obtained from the hu-BLT mice. Single cell suspensions were obtained by digesting tissues using DMEM medium supplemented with collagenase II (1mg/mL) (oral tumor) (Invitrogen, CA) and DNAse (10u/mL) (Sigma-Aldrich, CA) and 1%BSA. The digested tissues were passed through 70 μM filters (Fisher Scientific, CA) to obtain single-cell suspensions. To obtain single-cell suspensions from BM, femurs were flushed using media, and filtered through a 40 μm cell strainer. Spleens were removed and single-cell suspensions were prepared and filtered through a 40 μm cell strainer and centrifuged at 1500 rpm for 5 min at 4 °C. The pellets were then re-suspended in ACK buffer to remove the red blood cells. Murine peripheral blood mononuclear cells (PBMCs) were obtained using Ficoll-Hypaque centrifugation of heparinized blood specimens. The white, cloudy layer containing PBMCs was harvested, washed, and re-suspended in the RPMI 1640 media (Life Technologies, CA), supplemented with 10% FBS. Single-cell suspensions of each tissue were cultured in the presence and/or absence of IL-2 (1000 units/mL) treatment, using RPMI 1640 media (Life Technologies, CA), supplemented with 10% FBS.

Impedance Assay (eSight)

The xCELLigence RTCA eSight system (Agilent, USA) utilizes advanced impedance-based and image-based biosensor technology to dynamically analyze cell behavior and functions. Equipped with specialized E-Plates containing gold biosensors at the bottom of each well, the system offers a non-invasive means to continuously monitor cellular parameters such as proliferation, adhesion, morphology, migration, and differentiation. The process began by

establishing a background impedance measurement after adding the media. Target cells were then introduced at a concentration of $5x10^3$ cells per well. The system operated overnight for target cell attachment, capturing impedance measurements every 15 minutes and images hourly. After 24 hours, effector cells were added in a sequence of serial dilutions starting at a 2.5:1 effector-to-target (E:T) ratio, reducing through several stages down to a 0.625:1. The system then continued to monitor these interactions through impedance and visual data for an extended period of 72 hours, providing detailed insights into cell dynamics.

Statistical analysis

A one-tailed, unpaired Student t-test was conducted for statistical analysis. To compare different groups, one-way ANOVA with a Bonferroni post-test was employed. Cytotoxicity and cytokine analysis were performed using duplicate or triplicate samples for assessment. The levels of statistical significance are represented by the following symbols: ***(p-value < 0.001), **(p-value 0.001-0.01), *(p-value 0.01-0.05).

Results

Chapter 1: Establish the functional differences between super-charged NKs (sNK) expanded through live and sonicated osteoclasts.

Live osteoclast expanded sNK mediate higher direct cytotoxicity than sonicated osteoclast expanded sNK.

On day 9 of NK expansion through both methods, the sNK were tested in the ^{51}Chromium release assay to evaluate their cytotoxicity over the 4-hour incubation period. OC-expanded sNK cells showed higher cytotoxicity against OSCSC than sOC-expanded sNK cells (fig. 1).

To gain a deeper insight in terms of the cytotoxicity of both sNK cells, eSight was employed to evaluate the cellular dynamics over 48-hour co-culture. Pictures were taken at 0 hour, 24-hour, 48-hour co-culture show the comparison of OC and sOC-expanded sNK cells, where OC-expanded sNK shows most eradication of OSCSC by 48 hours (fig. 2A, B). Cell Index results indicate that OC-expanded sNK was able to halt the development of OSCSC, while sOC-expanded sNK could not match the counterpart's performance (fig. 3A). The percent cytolysis of OC-expanded sNK reached almost 60% within 24 hours, while sOC-expanded sNK reached only about 30% at the same time point. (fig. 3B).

Live-osteoclast expanded sNK has higher IFN-γ secretion than Sonicated-osteoclast expanded sNK

Besides their role in mediating cytotoxicity against tumor cells, NK cells are critical in halting cancer progression by secreting cytokines, particularly IFN-γ. IFN-γ has been shown to

differentiate cancer stem cells [37]. This differentiation leads to reduced tumor growth and increased sensitivity of cancer cells to chemotherapeutic drugs. To assess IFN-γ levels, the supernatant from sNK cell cultures was analyzed using ELISA, providing insights into the overall population's cytokine secretion on day 15. A greater level of IFN-γ was detected in the supernatant from OC-expanded sNK cells than that from sOC-expanded sNK cells (Fig. 4).

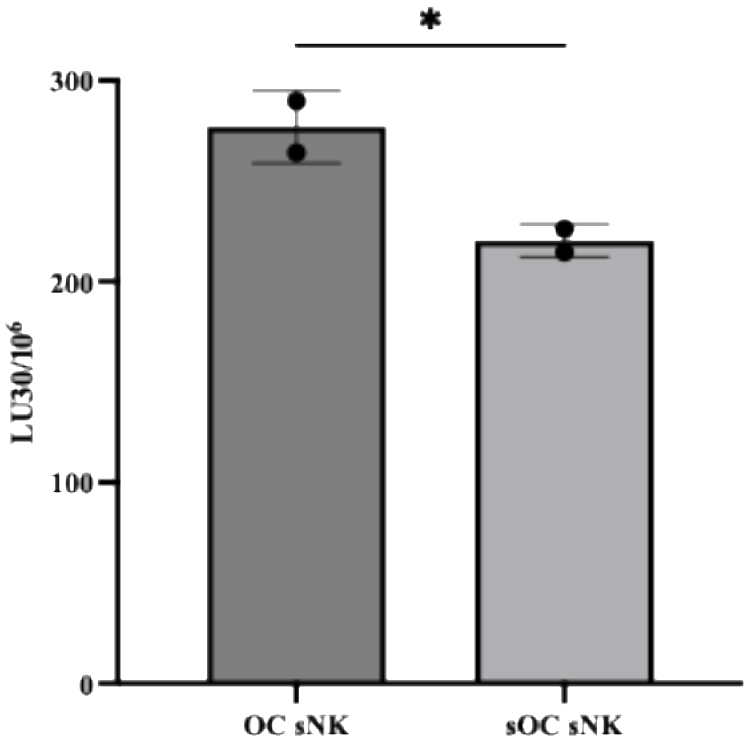

Figure 1: The cytotoxic effectiveness of sNK cells expanded using live and sonicated osteoclasts as determined by the ^{51}Chromium release assay. The lytic units 30/10^6 cells were calculated using the inverse number of NK cells required to lyse 30% of OSCSCs multiplied by 100. The following symbols represent the levels of statistical significance within each analysis, ***(p-value <0.001), **(p-value 0.001-0.01), *(p-value 0.01–0.05).

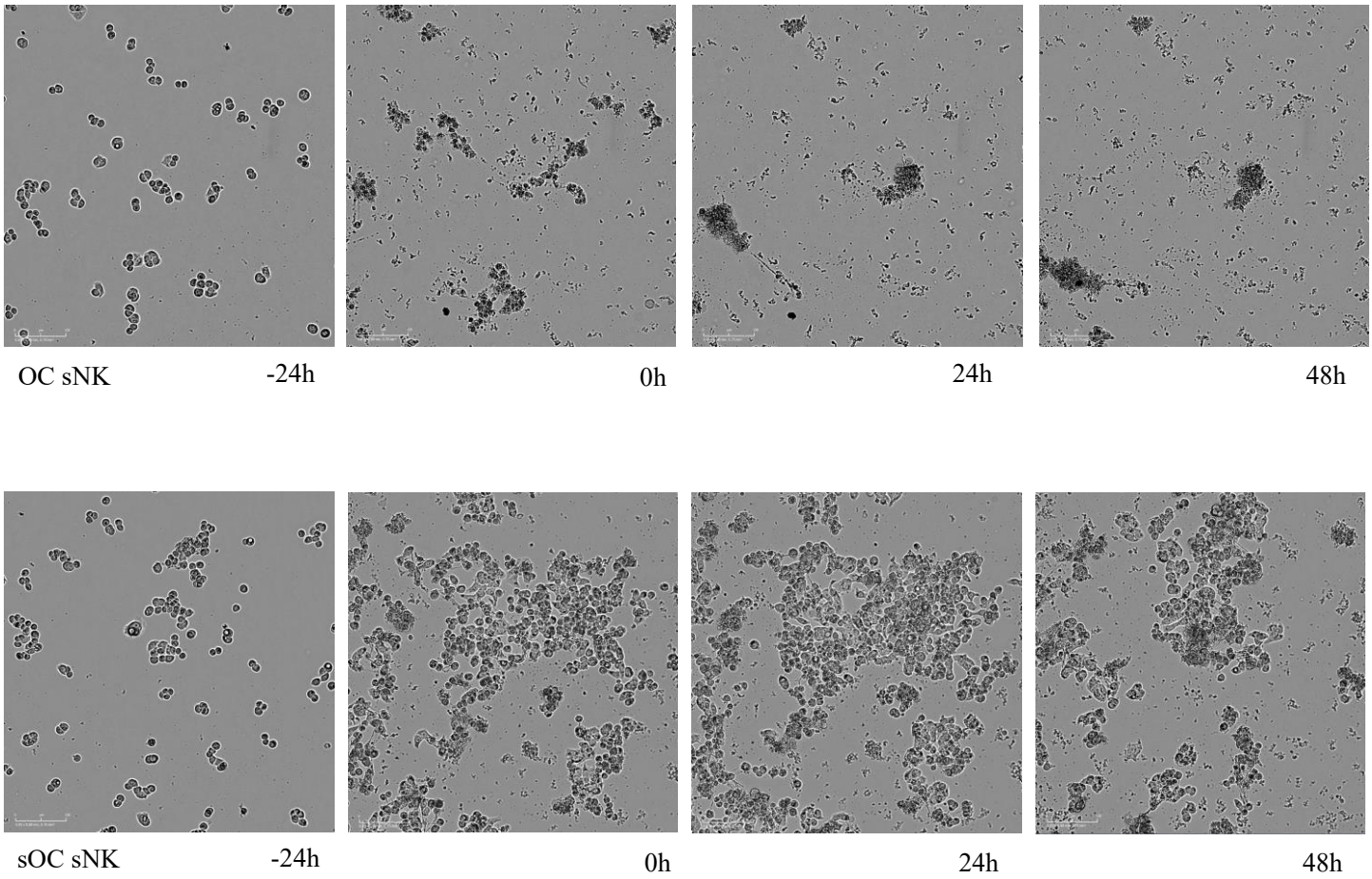

Figure 2: Real-time cytotoxicity monitoring of sNK cells expanded through OC (A) and sOC (B) against OSCSC using eSight. Images were captured at 24 hours before the addition of effector cells, at 0 hours, at 24 hours, and at 48 hours during the co-culture period.

A

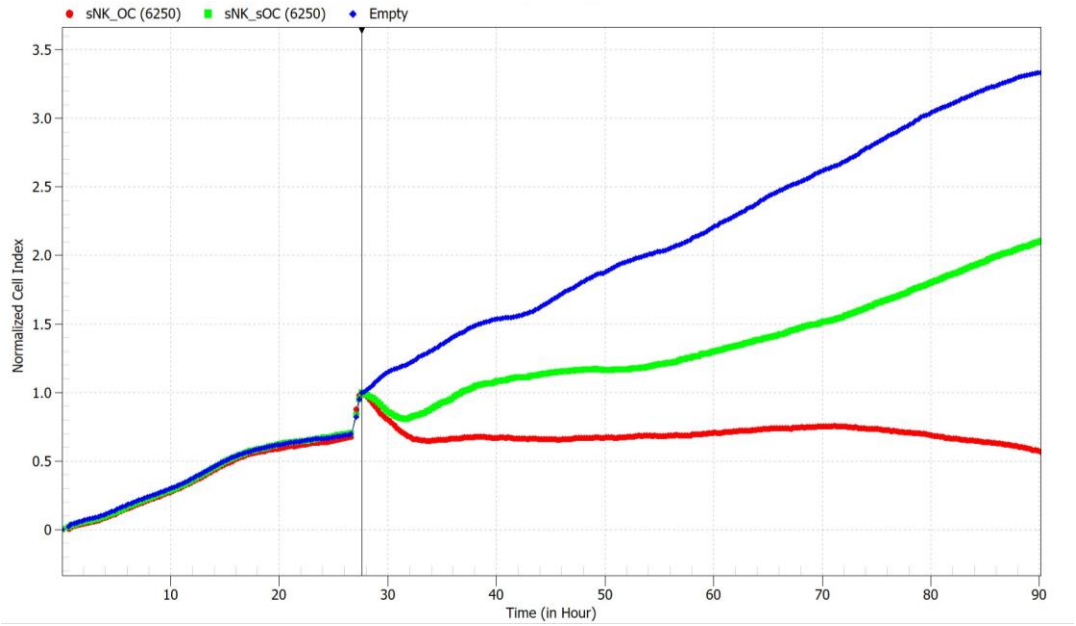

B

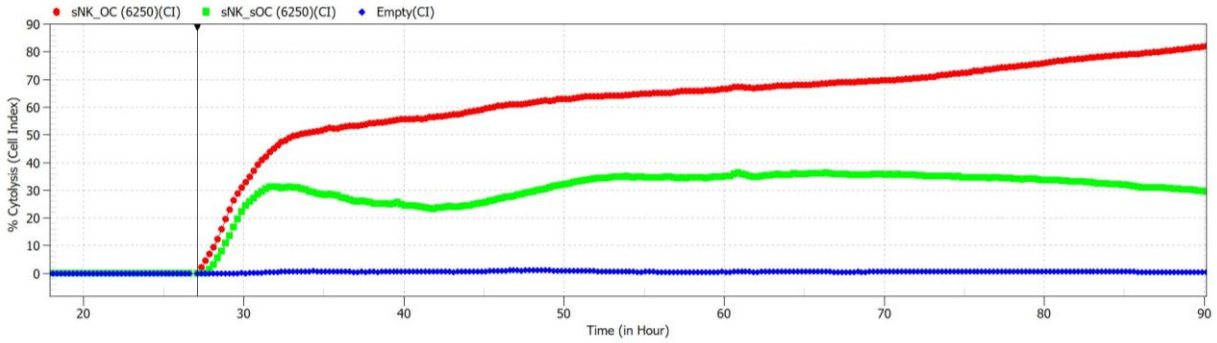

Figure 3: Scatter Plots from the eSight assay depicting the cytotoxic activity of sNK cells expanded with live (red) and sonicated osteoclasts (green) against OSCSCs (blue) over 72 hours. E:T ratio shown is 0.625:1. The cell index over 90 hours, normalized time at 0 hour (A). The percent cytolysis of both sNK cells against OSCSC (B).

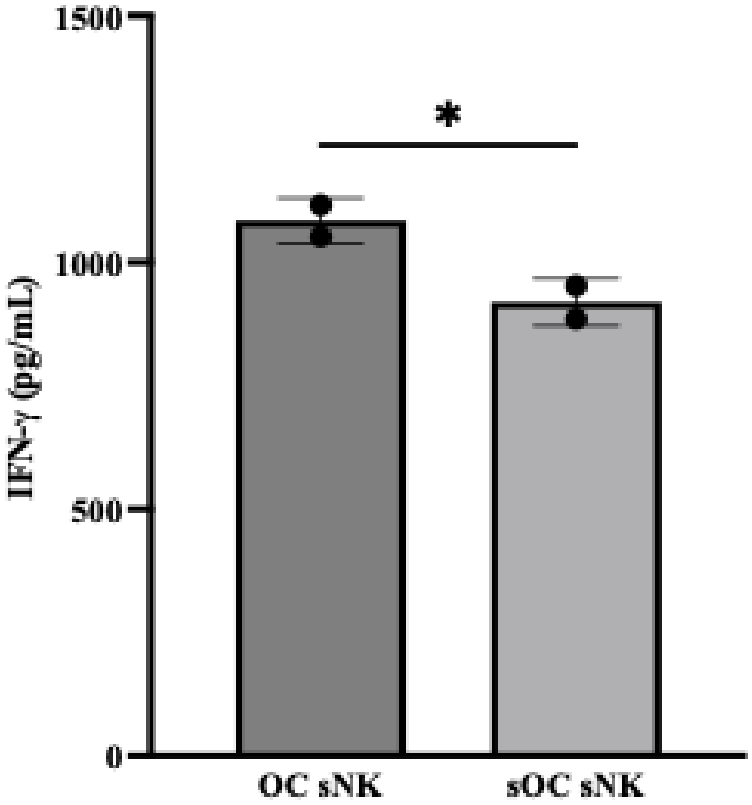

Figure 4: IFN-γ secretion levels in super-charged NK (sNK) cells expanded through live osteoclasts (OC) and sonicated osteoclasts (sOC). The supernatant from sNK cell cultures was collected on day 15 and analyzed using ELISA. The bar graph illustrates the concentration of IFN-γ (pg/mL) in the supernatant, comparing the levels of IFN-γ in OC-expanded sNK cells and sOC-expanded sNK cells. Error bars represent the standard deviation (SD) of triplicate samples. The following symbols represent the levels of statistical significance within each analysis, ***(p-value <0.001), **(p-value 0.001-0.01), *(p-value 0.01–0.05).

Discussion

In the exploration of supercharged NK (sNK) cell functional differences when expanded through live and sonicated osteoclasts, several key findings were observed.

The cytotoxic capabilities of these sNK cells were assessed using a ^{51}Chromium release assay and further analyzed through the eSight system over a 48-hour period. Results indicated that NK cells expanded with live osteoclasts exhibited superior cytotoxicity and were more effective in eliminating OSCSC, reaching almost 80% eradication within 24 hours at the 0.625:1 effector-to-target (E:T) ratio. This enhanced cytotoxic response was accompanied by higher IFN-γ secretion levels, as measured by ELISA, suggesting a stronger immunomodulatory impact on tumor cell suppression. The greater IFN-γ output not only signifies more effective direct cell lysis but also implies potential benefits in sensitizing cancer cells to chemotherapeutic agents and inhibiting tumor progression through immune-mediated mechanisms.

Overall, the differences in expansion methods significantly impact the efficacy of sNK cells, with live osteoclasts fostering a more potent cytotoxic and immunoregulatory response. These findings contribute to a better understanding of the potential of sonicated osteoclasts expanded sNK cells in therapeutic applications.

Chapter 2: To investigate and compare the lysing capacity of supercharged NK (sNK) cells and primary NK cells against Uterine Cancer Stem-like and Differentiated Cell Lines AN3CA and HEC-1B

AN3CA cells exhibit a higher growth rate in comparison to HEC-1B cells

The growth of AN3CA and HEC-1B cells was assessed by plating $1x10^5$ cells per well in a 6-well culture dish. One well was trypsinized and counted every 24 hours using microscopy. AN3CA cells exhibited a higher growth rate compared to HEC-1B cells (fig. 5), consistent with their poorly differentiated and more aggressive nature. This observation aligns with the expected behavior of poorly differentiated cancer cells, which typically demonstrate rapid proliferation.

sNK cells exhibit higher cytotoxicity against AN3CA cells

In previous studies, we determined that sNK cells exhibit higher cytotoxicity against poorly differentiated cancer cells. To further investigate, we performed a 4-hour ^{51}Cr release assay to evaluate sNK cell performance in lysing AN3CA and HEC-1B cells, with OSCSC serving as a control, representing a stem-like cancer cell line. sNK cells exhibited high cytotoxicity against AN3CA cells, similar to their performance against OSCSC (fig. 6). This suggests that sNK cells are particularly effective against poorly differentiated cancer cells. sNK cells showed lower cytotoxicity against HEC-1B cells, which are more differentiated. This aligns with our hypothesis and previous findings that sNK cells are more potent against less differentiated, more aggressive cancer cells.

These results were further corroborated by eSight real-time cytotoxicity monitoring. Over a 72-hour co-culture period, images captured at 24-hour intervals demonstrated that sNK cells were able to significantly reduce the viability of AN3CA cells, while the impact on HEC-1B cells was markedly less pronounced (fig. 7A, B). The real-time monitoring provided dynamic evidence of the cytotoxic process, with sNK cells visibly reducing the number of viable AN3CA cells over time.

sNK cells exhibit higher cytotoxicity than treated pNK cells

Previous studies have shown that pNK cells treated with IL-2 or IL-2 combined with sAJ4 exhibit higher cytotoxicity than untreated NK cells. To evaluate the cytotoxicity of these treated pNK cells in comparison to sNK cells, we performed a ^{51}Cr release assay and eSight real-time cytotoxicity monitoring with AN3, HEC-1B, and OSCSC as target cells. sNK cells demonstrated superior killing ability compared to pNK cells, regardless of the treatment with IL-2 or IL-2+sAJ4 (fig. 8). sNK cells showed a greater reduction in cell index over time when co-cultured with AN3CA and OSCSC cells compared to pNK cells treated with IL-2 or IL-2+sAJ4 (fig. 9A-C). The cell index for HEC-1B cells showed a less pronounced reduction, consistent with the lower cytotoxicity observed. sNK cells achieved higher % cytolysis across all three cell lines, with the most significant impact on AN3CA and OSCSC cells (fig. 10A-C). IL-2+sAJ4 treated pNK cells showed improved cytolysis compared to IL-2 treated pNK cells, but did not match the efficacy of sNK cells. This reinforces the enhanced efficacy of sNK cells in targeting and lysing cancer cells.

The findings highlight the cytotoxic capabilities of sNK cells against poorly differentiated cancer cells like AN3CA, surpassing the performance of treated pNK cells. The data suggest that

osteoclast expansion and subsequent activation of sNK cells significantly enhance their therapeutic potential.

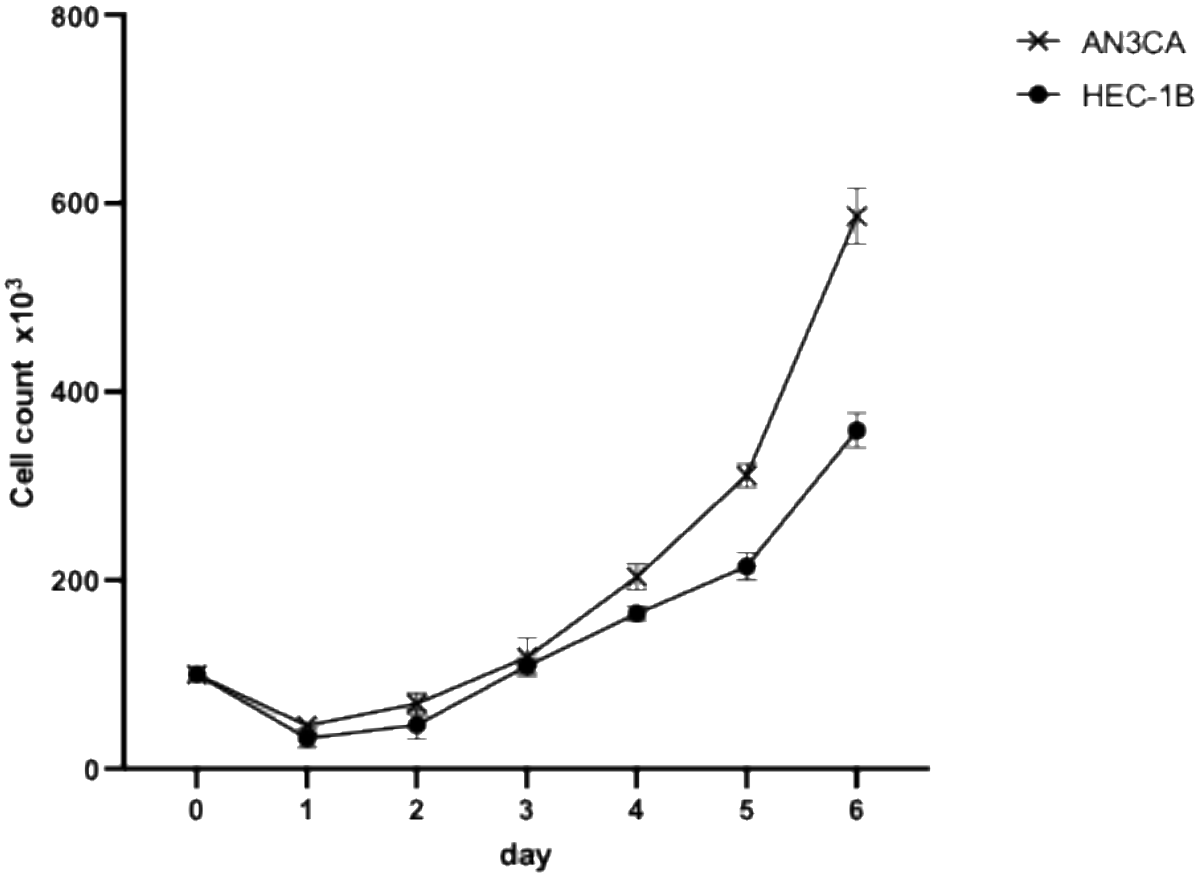

Figure 5: Growth rate of AN3CA and HEC-1B cells. AN3CA and HEC-1B cells were plated at a density of $1x10^5$ cells per well in a 6-well culture dish. Cell counts were taken every 24 hours using microscopy to assess growth rates. The scatter plot compares the growth rate of AN3CA cells and HEC-1B cells. Error bars represent the standard deviation (SD) of triplicate samples.

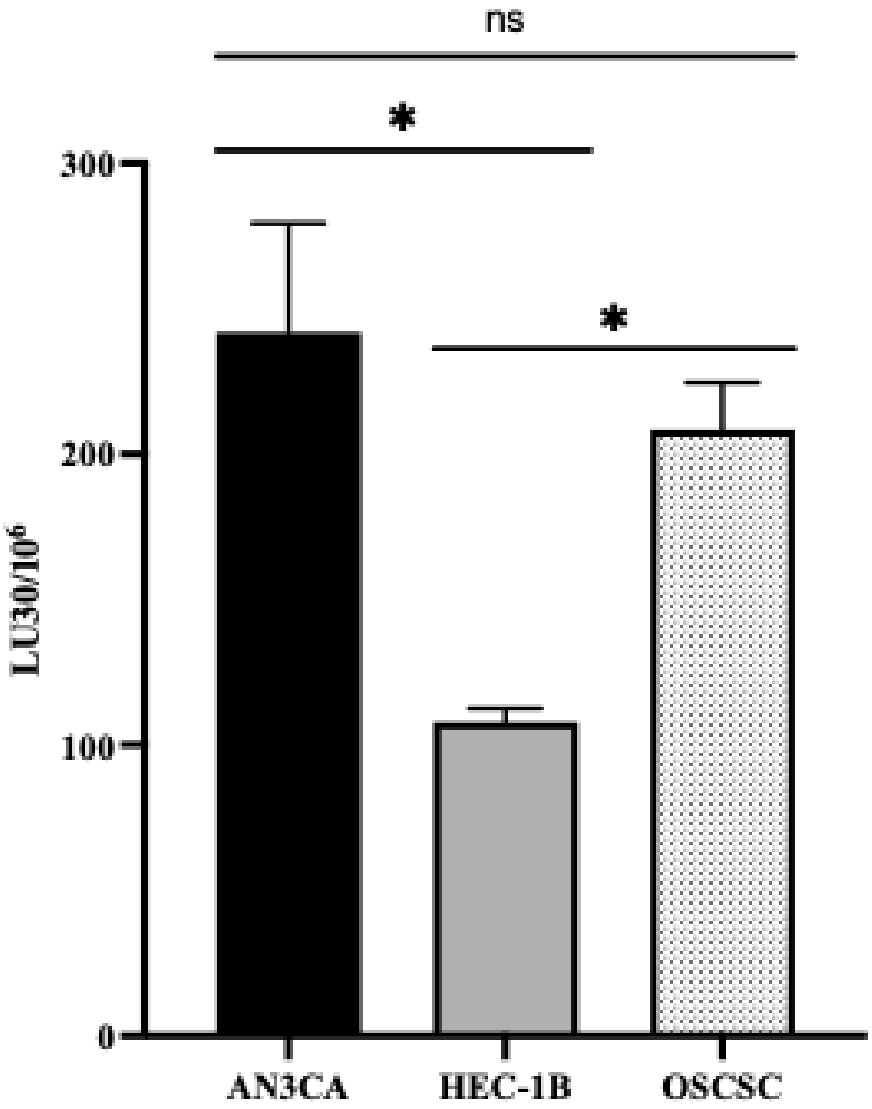

Figure 6: Cytotoxicity of supercharged NK (sNK) cells against AN3CA and HEC-1B cells. A 4-hour ^{51}Cr release assay was performed to evaluate the cytotoxicity of sNK cells against AN3CA and HEC-1B cells, with OSCSC serving as a control representing a stem-like cancer cell line. The lytic units 30/10^6 cells were calculated using the inverse number of NK cells required to lyse 30% of OSCSCs multiplied by 100. The following symbols represent the levels of statistical significance within each analysis, ***(p-value <0.001), **(p-value 0.001-0.01), *(p-value 0.01–0.05).

A

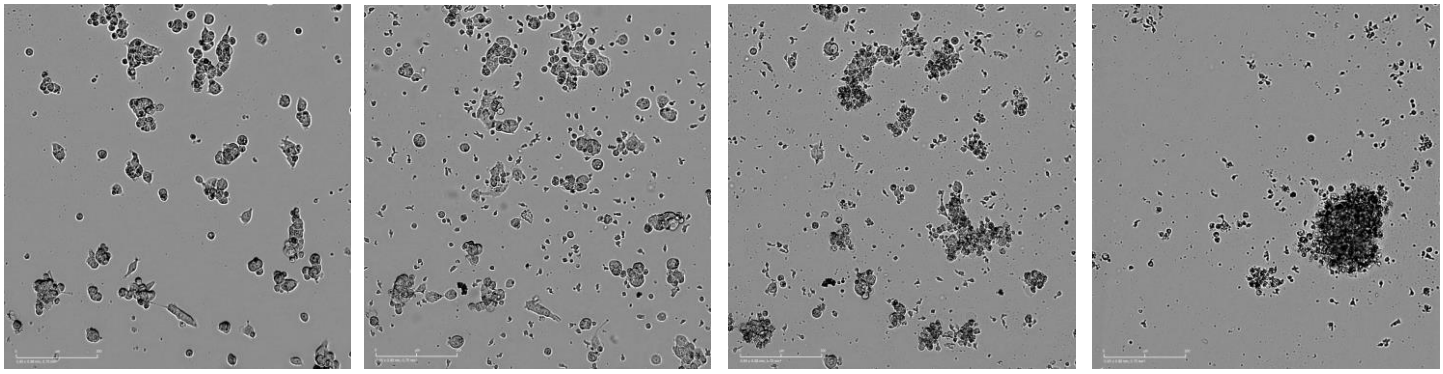

B

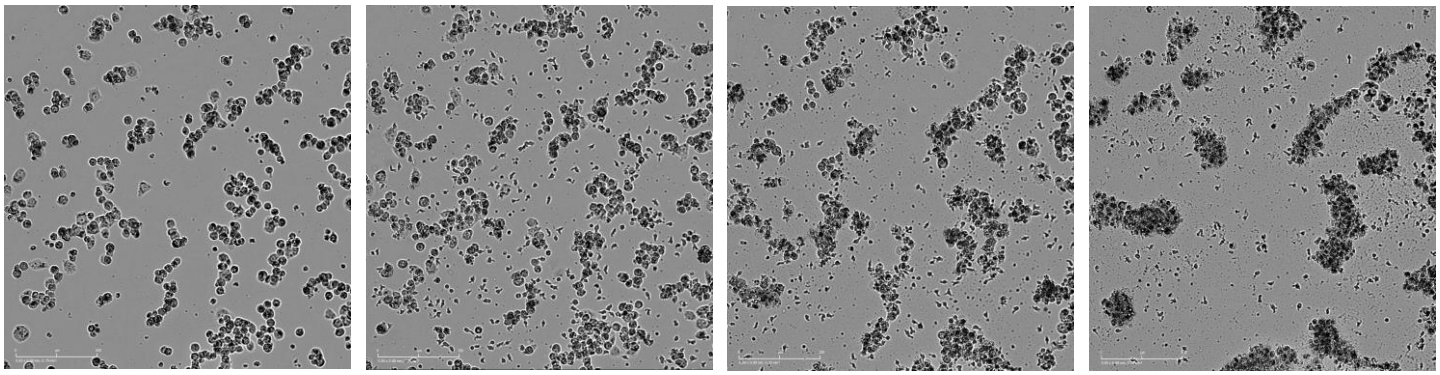

Figure 7: Real-time cytotoxicity monitoring of supercharged NK (sNK) cells against AN3CA and HEC-1B cells using eSight. Panel (A) shows images of AN3CA cells, and Panel (B) shows images of HEC-1B cells, both captured at 24-hour intervals over a 72-hour co-culture period.

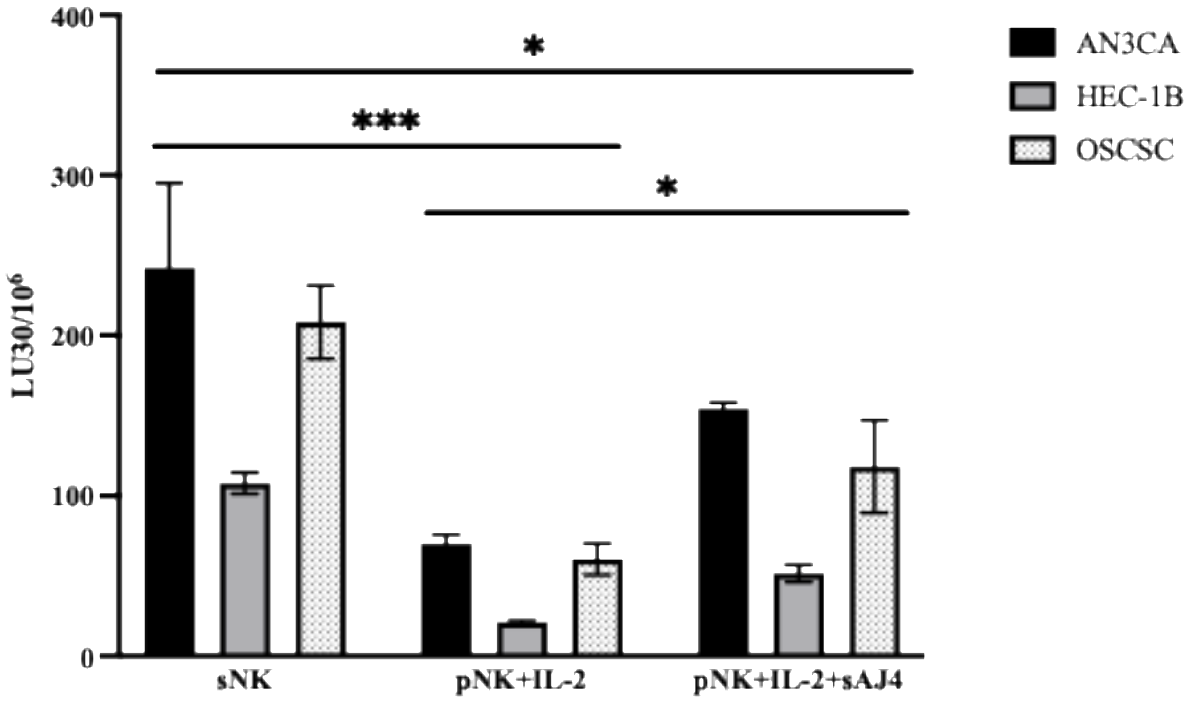

Figure 8: Comparative cytotoxicity of supercharged NK (sNK) cells and primary NK (pNK) cells treated with IL-2 or IL-2 combined with sAJ4 against AN3CA, HEC-1B, and OSCSC cells. A 4-hour ^{51}Cr release assay was performed to evaluate the cytotoxicity of these cells. The lytic units $30/10^6$ cells were calculated using the inverse number of NK cells required to lyse 30% of OSCSCs multiplied by 100. The following symbols represent the levels of statistical significance within each analysis, ***(p-value <0.001), **(p-value 0.001-0.01), *(p-value 0.01–0.05).

A

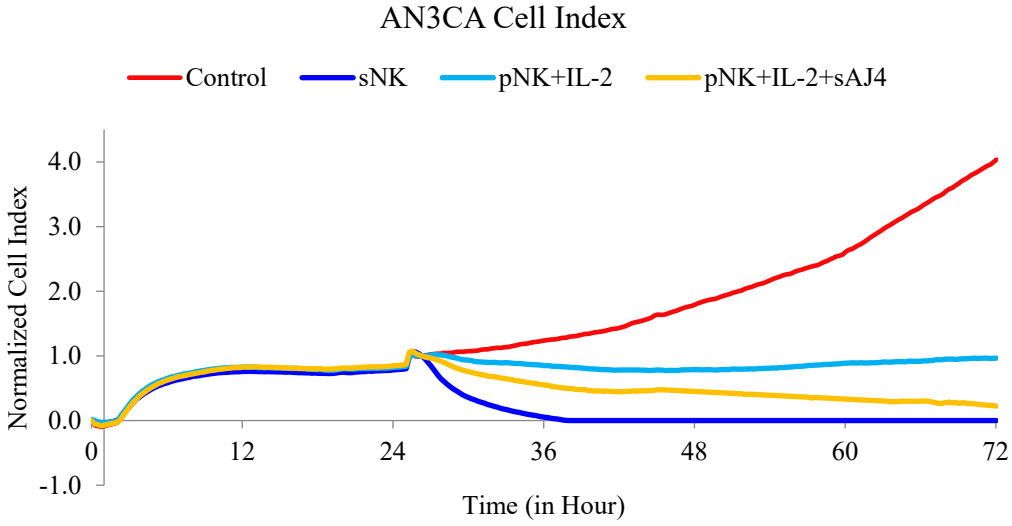
AN3CA Cell Index
Control
sNK
pNK+IL-2
pNK+IL-2+sAJ4
Normalized Cell Index
4.0
3.0
2.0
1.0
0.0
-1.0
0
12
24
36
48
60
72
Time (in Hour)

B

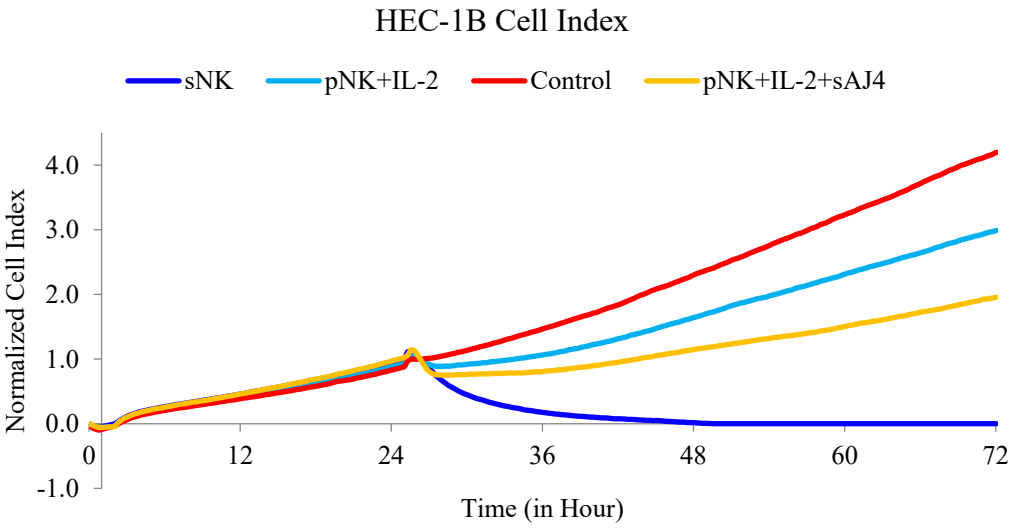
HEC-1B Cell Index
sNK
pNK+IL-2
Control
pNK+IL-2+sAJ4
Normalized Cell Index
4.0
3.0
2.0
1.0
0.0
-1.0
0
12
24
36
48
60
72
Time (in Hour)

C

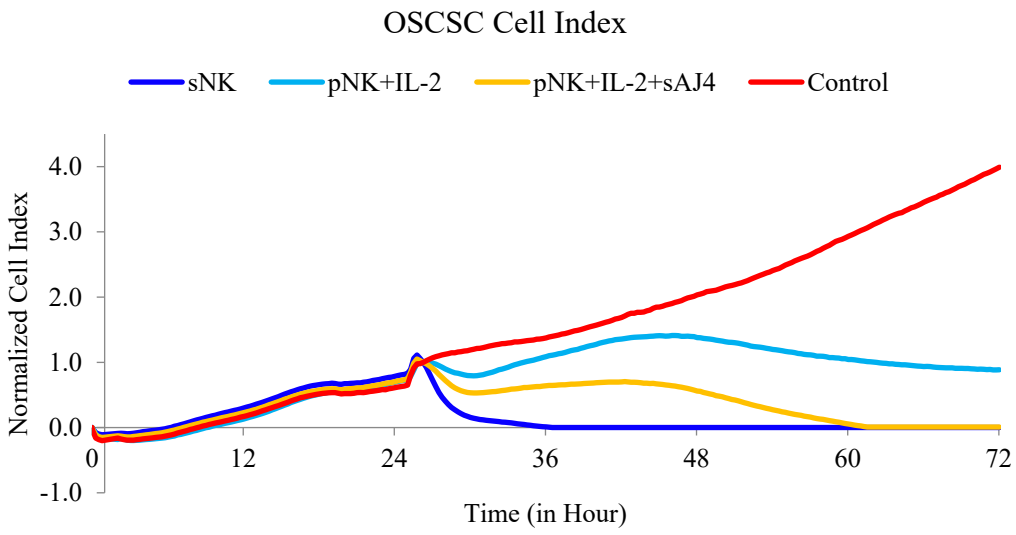
OSCSC Cell Index
sNK
pNK+IL-2
pNK+IL-2+sAJ4
Control
Normalized Cell Index
4.0
3.0
2.0
1.0
0.0
-1.0
0
12
24
36
48
60
72
Time (in Hour)

Figure 9: Real-time cytotoxicity monitoring of sNK (dark blue) cells and pNK cells treated with IL-2 (light blue) or IL-2 combined with sAJ4 (yellow) against AN3CA, HEC-1B, and OSCSC cells (red) using eSight. Panels (A), (B), and (C) show the change in cell index over a 72-hour co-culture period for AN3CA, HEC-1B, and OSCSC cells, respectively.

A

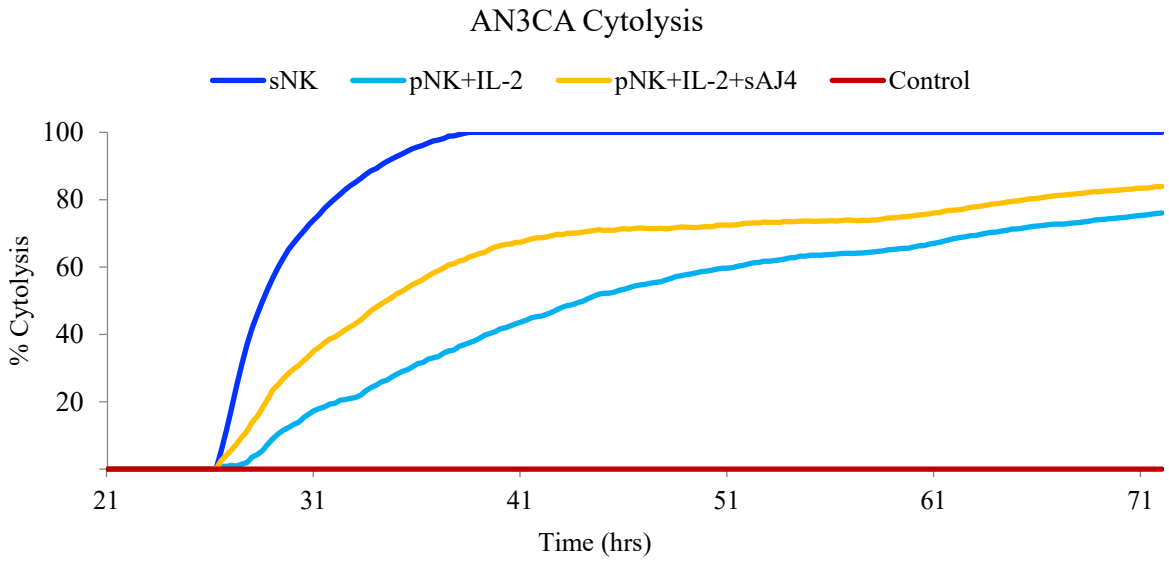
AN3CA Cytolysis
sNK
pNK+IL-2
pNK+IL-2+sAJ4
Control
% Cytolysis
100
80
60
40
20
21
31
41
51
61
71
Time (hrs)

B

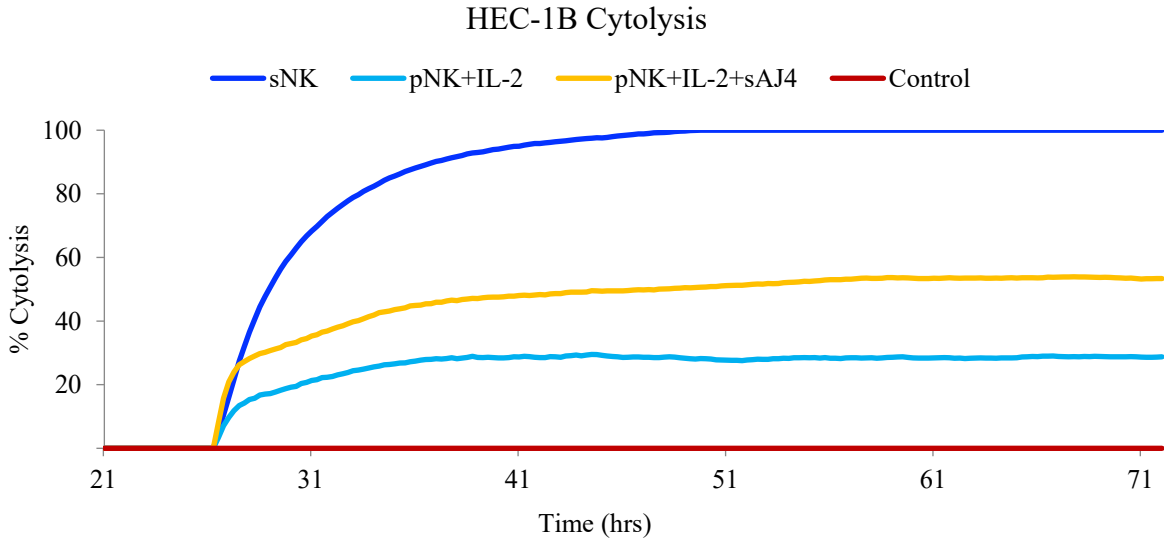
HEC-1B Cytolysis
sNK
pNK+IL-2
pNK+IL-2+sAJ4
Control
% Cytolysis
100
80
60
40
20
21
31
41
51
61
71
Time (hrs)

C

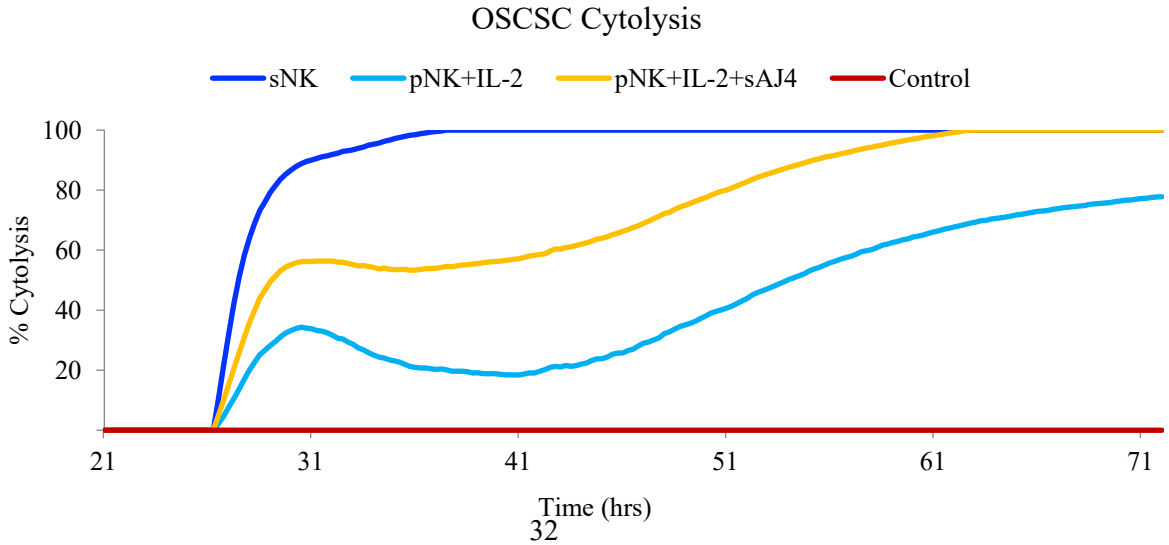
OSCSC Cytolysis
sNK
pNK+IL-2
pNK+IL-2+sAJ4
Control
% Cytolysis
100
80
60
40
20
21
31
41
51
61
71
Time (hrs)

Figure 10: Percentage cytolysis of supercharged NK (sNK) cells and primary NK (pNK) cells treated with IL-2 or IL-2 combined with sAJ4 against AN3CA, HEC-1B, and OSCSC cells. Panels (A), (B), and (C) show the % cytolysis over a 72-hour co-culture period for AN3CA, HEC-1B, and OSCSC cells, respectively.

Discussion

In this chapter, we explored the cytotoxic effects of supercharged NK (sNK) cells on two uterine cancer cell lines, AN3CA and HEC-1B, as well as a stem-like cancer cell line, OSCSC. Our findings provide valuable insights into the differential effectiveness of sNK cells against cancer cells with varying degrees of differentiation.

The initial growth rate assessment of AN3CA and HEC-1B cells revealed that AN3CA cells proliferate at a faster rate compared to HEC-1B cells. This is consistent with the poorly differentiated and aggressive nature of AN3CA cells. The rapid proliferation of AN3CA cells highlights their malignant potential and underscores the need for effective therapeutic strategies to target such aggressive cancer types.

Our 4-hour ^{51}Cr release assay demonstrated that sNK cells exhibit significantly higher cytotoxicity against AN3CA cells compared to HEC-1B cells. This higher cytotoxicity against AN3CA cells was on par with the cytotoxicity observed against OSCSC, a stem-like cancer cell line. These results suggest that sNK cells are particularly effective against poorly differentiated and stem-like cancer cells, which are typically more challenging to treat with conventional therapies.

The real-time cytotoxicity monitoring using eSight provided dynamic evidence supporting these findings. Over the 72-hour co-culture period, sNK cells significantly reduced the viability of AN3CA and OSCSC cells, while the impact on HEC-1B cells was less pronounced. The cell index and % cytolysis data further corroborated these observations, with sNK cells achieving higher % cytolysis across all three cell lines. The greatest cytolytic effect was observed against AN3CA and OSCSC cells, indicating the enhanced capability of sNK cells to target and eliminate poorly differentiated and stem-like cancer cells.

Previous studies have shown that pNK cells treated with IL-2 or IL-2 combined with sAJ4 exhibit higher cytotoxicity than untreated NK cells. Our ^{51}Cr release assay and eSight results confirm these findings, with treated pNK cells showing improved cytotoxicity compared to untreated pNK cells. However, even with these treatments, pNK cells did not match the efficacy of sNK cells.

The superior performance of sNK cells compared to treated pNK cells highlights the significant impact of osteoclast expansion on NK cell functionality. sNK cells, expanded through osteoclast co-culture, demonstrate enhanced cytotoxicity and the ability to target aggressive cancer cells.

Chapter 3: In Vivo Efficacy of sNK Cells in Targeting AN3CA Tumor Progression in huBLT mice

Decreased tumor burden huBLT mice treated with sNK cells

After the hu-BLT mice were sacrificed, endometrial tumors were resected. A comparative analysis showed that the tumors from mice treated with NK immunotherapy were visibly smaller (fig. 13A). Furthermore, these tumor's weight (fig. 13B) and volume (fig. 13C) decreased compared to those from the control group.

Increased IFN-γ secretion level after IL-2 treatment on PBMC of sNK treated group

Further analysis involved assessing the immune response via IFNγ production by PBMCs post-mortem after ex vivo IL-2 stimulation. The results show an increase in IFNγ levels in sNK-treated mice compared to controls (fig. 13D). This finding suggests that sNK cell treatment not only suppresses tumor growth but may also reinvigorate the immune system's capacity to combat cancer, potentially reversing tumor-induced immunosuppression.

A

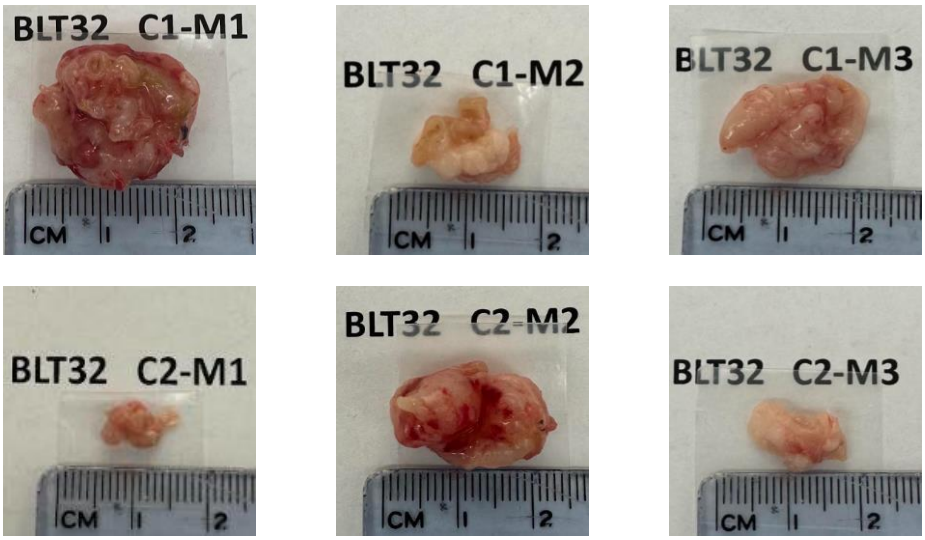
BLT32 C1-M1
BLT32 C1-M2
BLT32 C1-M3
BLT32 C2-M1
BLT32 C2-M2
BLT32 C2-M3
CM 1 2

B

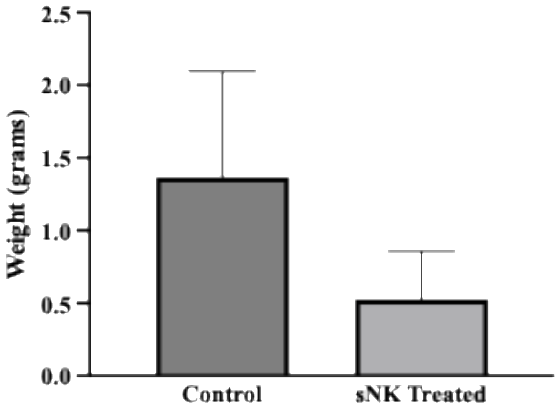
Weight (grams)
2.5
2.0
1.5
1.0
0.5
0.0
Control
sNK Treated

C

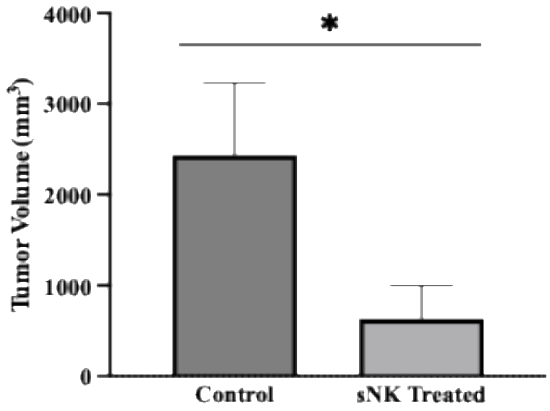
Tumor Volume (mm3)
4000
3000
2000
1000
0
*
Control
sNK Treated

D

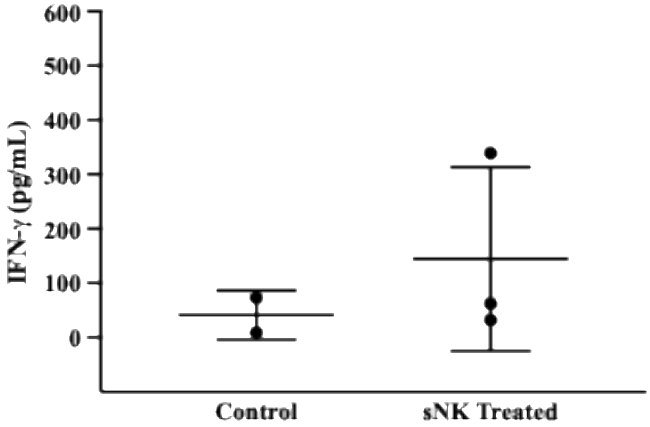
IFN-γ (pg/mL)
600
500
400
300
200
100
0
Control
sNK Treated

Figure 11: In vivo efficacy of supercharged NK (sNK) cells in targeting AN3CA tumor progression in huBLT mice. Comparison of resected endometrial tumors from huBLT mice treated with NK immunotherapy and control group (A). Tumor weight analysis of sNK-treated mice compared to the control group, measured in grams (B). Tumor volume analysis in sNK-treated mice relative to controls, measured in mm^3 (C). IFN-γ secretion levels (pg/mL) in PBMCs post-mortem after ex vivo IL-2 stimulation (D). The following symbols represent the levels of statistical significance within each analysis, ***(p-value <0.001), **(p-value 0.001-0.01), *(p-value 0.01–0.05).

Discussion

The substantial decrease in tumor volume among sNK-treated mice confirms the cells' potent cytotoxic capabilities. This supports the hypothesis that a well-maintained physiological environment during sNK cell cultivation is crucial for developing highly effective therapeutic agents. The observed efficacy suggests that sNK cells retain their functional integrity and aggressive anti-tumor properties in a live setting.

The increase in IFNγ production after ex vivo IL-2 stimulation of PBMCs is particularly significant. This indicates that sNK cell treatment extends beyond direct tumor cell cytotoxicity, modulating the systemic immune environment to counteract tumor-induced immunosuppression. IFNγ plays a vital role in enhancing both innate and adaptive immune responses, crucial for effective anti-tumor activity and potentially reducing recurrence and metastasis.

The dual action of sNK cells—direct cytotoxic effects against tumor cells and immunomodulatory effects enhancing systemic immunity—suggests their potential as a versatile and robust therapeutic option. Their applicability may extend across various cancer types, offering a broad therapeutic impact. The study's findings advocate for clinical trials exploring sNK cell therapies, focusing on optimizing therapeutic protocols to maximize benefits and minimize potential side effects.

Conclusion

This thesis provides an examination of the therapeutic potential of sNK cells, expanded through osteoclast co-culture, in uterine cancer models. The study aimed to elucidate the functional differences between sNK cells expanded using live and sonicated osteoclasts, assess their cytotoxic efficacy against poorly differentiated and well-differentiated uterine cancer cell lines, and evaluate their impact on tumor progression in huBLT mouse models.

Our findings revealed the successful expansion of sNK with sonicated osteoclasts. sNK cells expanded with live osteoclasts, however, demonstrated superior cytotoxicity and IFN-γ secretion.

In the context of cytotoxic efficacy against cancer cell lines, sNK cells exhibited significantly higher cytotoxicity against the poorly differentiated AN3CA cell line, akin to their effect on stem-like cancer cells (OSCSC). Conversely, sNK cells showed lower cytotoxicity against the more differentiated HEC-1B cell line. The performance of sNK cells was superior to that of pNK cells treated with IL-2 or IL-2+sAJ4, highlighting the enhanced effectiveness of osteoclast-expanded sNK cells.

In vivo studies using huBLT mouse models demonstrated that sNK cell treatment led to a substantial reduction in tumor burden, with significant decreases in tumor weight and volume compared to controls. Additionally, increased IFN-γ secretion levels in sNK-treated mice indicated a strengthened immune response, suggesting that sNK cells can potentially reverse tumor-induced immunosuppression and improve anti-tumor immunity.

These findings shed light on the therapeutic potential of sNK cells in targeting aggressive and poorly differentiated cancer cells. The enhanced cytotoxicity and immune-modulatory effects of sNK cells, particularly those expanded through live osteoclasts, present a promising

method for developing more effective cancer immunotherapies. Future research should focus on elucidating the molecular mechanisms underlying the enhanced functionality of sNK cells, exploring the clinical application and scalability of sNK cell-based therapies, and investigating the potential synergistic effects of combining sNK cells with other immunotherapies or chemotherapies to further enhance treatment efficacy.

In summary, this thesis contributes to the growing body of evidence supporting the use of sNK cells in cancer treatment, offering new insights and potential strategies for improving therapeutic outcomes for patients with aggressive cancers.

References

1. Vivier, E., Tomasello, E., Baratin, M., Walzer, T., & Ugolini, S. (2008). Functions of natural killer cells. Nature immunology, 9(5), 503-510.
2. Hashemi, E., & Malarkannan, S. (2020). Tissue-resident NK cells: development, maturation, and clinical relevance. Cancers, 12(6), 1553.
3. Jewett A, Man Y-G, Tseng H-C. Dual Functions of Natural Killer Cells in Selection and Differentiation of Stem Cells; Role in Regulation of Inflammation and Regeneration of Tissues. Journal of Cancer. 2013;4(1):12-24.
4. Wang, W., Erbe, A. K., Hank, J. A., Morris, Z. S., & Sondel, P. M. (2015). NK cell mediated antibody-dependent cellular cytotoxicity in cancer immunotherapy. Frontiers in immunology, 6, 368.
5. Lanier, L.L., NK cell recognition. Annu Rev Immunol, 2005. 23: p. 225-74
6. Perera Molligoda Arachchige, A. S. (2021). Human NK cells: From development to effector functions. Innate Immunity, 27(3), 212-229.
7. Poli, A., Michel, T., Thérésine, M., Andrès, E., Hentges, F., & Zimmer, J. (2009). CD56bright natural killer (NK) cells: an important NK cell subset. Immunology, 126(4), 458-465.
8. Jordan S., & Zuhair, K. Natural killer cells in human health and disease. Clinical Immunology. 2006; 118 (1):1-10.
9. Amant, F., Moerman, P., Neven, P., Timmerman, D., Limbergen, E., & Vergote, I. (2005). Endometrial cancer. The Lancet, 366(9484), 491–505.
10. Crosbie, E., Kitson, S., McAlpine, J. N., Mukhopadhyay, A., Powell, M., & Singh, N. (2022). Endometrial cancer. The Lancet, 399(10333), 1412–1428.

11. Felix, A.S., Weissfeld, J.L., Stone, R.A. et al. Factors associated with Type I and Type II endometrial cancer. Cancer Causes Control 21, 1851–1856 (2010).
12. Xue, Q., Che, W., Xue, L., Zhang, X., Wang, X., & Lyu, J. (2023). Causes of death in endometrial cancer survivors: A Surveillance, Epidemiology, and End Result–based analysis. Cancer Medicine, 12(9), 10917–10930.
13. Chen, P.-C. (n.d.). The resistance of super charged NK cells to immunosuppression in tumor microenvironment (thesis). The Resistance of Super Charged NK Cells to Immunosuppression in Tumor Microenvironment.
14. Wang, Y., Yang, D., Cogdell, D., Hu, L., Xue, F., Broaddus, R., & Zhang, W. (2010). Genomic characterization of gene copy-number aberrations in endometrial carcinoma cell lines derived from endometrioid-type endometrial adenocarcinoma. Technology in cancer research & treatment, 9(2), 179–189.
15. Sillem, M., Prifti, S., Koumouridis, A., & Runnebaum, B. (1999). Invasiveness corresponds to differentiation rather than to proteinase secretion in endometrial cancer cell lines. European journal of gynaecological oncology, 20(5-6), 367–370.
16. AN3 CA - HTB-111 | ATCC. (n.d.). https://www.atcc.org/products/htb-111
17. HEC-1-B - HTB-113 | ATCC. (n.d.). https://www.atcc.org/products/htb-113
18. Simonet, W.S., et al., Osteoprotegerin: a novel secreted protein involved in the regulation of bone density., in Cell. 1997. p. 89(2): p. 309-19.
19. Burgess, T.L., et al., The ligand for osteoprotegerin (OPGL) directly activates mature osteoclasts. , in J Cell Biol. 1999. p. 145(3): p. 527-38.
20. Boyle, W.J., W.S. Simonet, and D.L. Lacey, Osteoclast differentiation and activation., in Nature. 2003. p. 423(6937): p. 337-42.

21. Popoff, S.N., et al., Coexistence of reduced function of natural killer cells and osteoclasts in two distinct osteopetrotic mutations in the rat. , in J Bone Miner Res. 1991. p. 6(3): p. 263-71. Lanier, L.L., NK cell receptors. Annu Rev Immunol, 1998. 16: p. 359-93.
22. Tseng, H.C., et al., Bisphosphonate-induced differential modulation of immune cell. function in gingiva and bone marrow in vivo: role in osteoclast-mediated NK cell activation. Oncotarget, 2015. 6(24): p. 20002-25. Kaur, K.; Cook, J.; Park, S.H.; Topchyan, P.; Kozlowska, A.; Ohanian, N.; Fang, C.;
23. Nishimura, I.; Jewett, A.Novel strategy to expand super-charged NK cells with significant potential to lyse and differentiate cancer stem cells: Differences in NK expansion and function between healthy and cancer patients. Front. Immunol. 2017, 8, doi:10.3389/fimmu.2017.00297.
24. Jewett, A.; Kos, J.; Kaur, K.; Turnsek, T.L.; Breznik, B.; Senjor, E.; Wong, P.; Nguyen, K.Y.; Ko, M.-W.Multiple Defects of Natural Killer Cells in Cancer Patients: Anarchy, Dysregulated Systemic Immunity, and Immunosuppression in Metastatic Cancer. Crit. Rev. Immunol. 2020, 40, 93–133, doi:10.1615/CRITREVIMMUNOL.2020033391.
25. Tseng HC, Arasteh A, Paranjpe A, Teruel A, Yang W, Behel A, Alva JA, Walter G, Head C, Jewett A, et al., Increased Lysis of Stem Cells but Not Their Differentiated Cells by Natural Killer Cells; De-Differentiation or Reprogramming Activates NK Cells. *Plos One*. 2010;5(7):e11590. doi: 10.1371/journal.pone.0011590. Shultz, L.D., et al., Human cancer growth and therapy in immunodeficient mouse models. Cold Spring Harb Protoc, 2014. 2014(7): p. 694-708.
26. Kozlowska, A.K., et al., Adoptive transfer of osteoclast-expanded natural killer cells for immunotherapy targeting cancer stem-like cells in humanized mice. Cancer Immunology,

Immunotherapy, 2016. 65(7): p. 835-845.

27. McDermott, S.P., et al., Comparison of human cord blood engraftment between immunocompromised mouse strains. Blood, 2010. 116(2): p. 193-200.
28. Brehm, M.A., et al., Parameters for establishing humanized mouse models to study human immunity: analysis of human hematopoietic stem cell engraftment in three immunodeficient strains of mice bearing the IL2rgamma(null) mutation. Clin Immunol, 2010. 135(1): p. 84-98.
29. Shultz, L.D., F. Ishikawa, and D.L. Greiner, Humanized mice in translational biomedical research. Nat Rev Immunol, 2007. 7(2): p. 118-30.
30. Ito, A., et al., Defucosylated anti-CCR4 monoclonal antibody exercises potent ADCC mediated antitumor effect in the novel tumor-bearing humanized NOD/Shi-scid, IL-2Rgamma(null) mouse model. Cancer Immunol Immunother, 2009. 58(8): p. 1195-206.
31. King, M.A., et al., Human peripheral blood leucocyte non-obese diabetic-severe combined immunodeficiency interleukin-2 receptor gamma chain gene mouse model of xenogeneic graft-versus-host-like disease and the role of host major histocompatibility complex. Clin Exp Immunol, 2009. 157(1): p. 104-18.
32. Shultz, L.D., et al., Humanized mice for immune system investigation: progress, promise and challenges. Nat Rev Immunol, 2012. 12(11): p. 786-98.
33. Shimizu, S., et al., A highly efficient short hairpin RNA potently down-regulates CCR5 expression in systemic lymphoid organs in the hu-BLT mouse model. Blood, 2010. 115(8): p. 1534-44.
34. Stoddart, C.A., et al., Superior human leukocyte reconstitution and susceptibility to vaginal HIV transmission in humanized NOD-scid IL-2Rgamma(-/-) (NSG) BLT mice. Virology,

2011. 417(1): p. 154-60.

35. Vatakis, D.N.; Koya, R.C.; Nixon, C.C.; Wei, L.; Kim, S.G.; Avancena, P.; Bristol, G.; Baltimore, D.; Kohn, D.B.; Ribas, A.; et al.Antitumor activity from antigen-specific CD8 T cells generated in vivo from genetically engineered human hematopoietic stem cells. Proc. Natl. Acad. Sci. 2011, 108, E1408–E1416, doi:10.1073/PNAS.1115050108.
36. Shimizu, S.; Hong, P.; Arumugam, B.; Pokomo, L.; Boyer, J.; Koizumi, N.; Kittipongdaja, P.; Chen, A.; Bristol, G.; Galic, Z.; et al.A highly efficient short hairpin RNA potently down-regulates CCR5 expression in systemic lymphoid organs in the hu-BLT mouse model. Blood 2010, 115, 1534–1544, doi:10.1182/BLOOD-2009-04-215855.
37. Kaur, K.; Cook, J.; Park, S.H.; Topchyan, P.; Kozlowska, A.; Ohanian, N.; Fang, C.; Nishimura, I.; Jewett, A.Novel strategy to expand super-charged NK cells with significant potential to lyse and differentiate cancer stem cells: Differences in NK expansion and function between healthy and cancer patients. *Front. Immunol.* 2017, *8*, doi:10.3389/fimmu.2017.00297.